Indian Journal of Fibre& Textile Research
Vol. 50, March 2025, pp. 7-14
DOI: 10.56042/ijftr.v50i1.5236

Weave design and formability of 3D textile preforms for composite applications

Ashwini Kumar Dash[1,a], Sameer Kumar Behera[2] & Bijoya Kumar Behera[3]

[1]Department of Textile Engineering, Odisha University of Technology and Research, Bhubaneswar 751 029, India
[2]School of Interdisciplinary Research, [3]Department of Textile and Fibre Engineering, Indian Institute of Technology Delhi, New Delhi 110 016, India

Received 29 August 2023; revised received and accepted 1 February 2024

Formability is a critical parameter in composite applications, determining a fabric's ability to attain a desired shape. This study evaluates the formability of 3D woven solid structures by analysing their forming energy. Orthogonal and interlock fabrics with six different weave designs are examined, revealing that bending rigidity serves as a reliable indicator of formability, as previously established for 2D graphite fibre preforms. A strong correlation is observed between forming energy and bending rigidity, with fabric crossover points playing a significant role in influencing both parameters. Notably, the correlation between crossover points and bending rigidity is found to be stronger than that with forming energy.

Keywords: Bending rigidity, Crossover points, Fabric formability, Interlock structure, Orthogonal structure

1 Introduction

Formability refers to a material's ability to adapt to a desired shape or geometry. In metals, formability is primarily determined by their elastic and plastic behaviour. However, in textile fabrics, formability is complex and is predominantly governed by the type of constituent fibres and textile architectures. Fabrics with good formability characteristics require less applied force and thus consume less energy in the forming process. Lindberg *et al.*[1] investigated a specific fabric property that determines the extent of compression before buckling. He termed this property "formability", which is the product of compressibility and bending rigidity- an essential criterion in garment construction. Extensibility can be considered analogousto longitudinal compressibility under low-stress applications, as measuring fabric compressibility before buckling is challenging[2]. Several researchers have explored fabric formability by varying aesthetic and mechanical parameters[3-8]. Consequently, formability has been recognised as a crucial factor for fabrics intended for apparel applications[9-11].

In composites, textile reinforcements have gained significant attention due to their superior shaping characteristics compared to laminates[12]. Two-dimensional (2D) textile materials can be more easily formed into three-dimensional (3D) shapes than unidirectional reinforcements[13]. Most available literature focuses on the forming behaviour of 2D textile preforms[14-17]. However, 3D textiles offer significant advantages as reinforcements in composite applications due to their substantial thickness and integrated structures[18-19]. These textiles are categorisedinto solid structures (for load-bearing applications),hollow structures (for lightweight structural composites), profiled structures (for machine components), and complex structures (for speciality textile composites). Chen *et al.*[20] illustrated a comprehensive overview of 3D textile woven structures for composite applications. The formability of this kind of fabric preform is also an important criterion for ascertaining multi-curvature shape formation for the same applications. Yu *et al.*[21] and Cai *et al.*[22] defined forming energy as one of the measuring indexes to determine the ability of a reinforcement to attain a desired shape. They further investigated dominant experimental parameters that show the closest relation to the forming energy by analysing different weave designs of 2D fabrics.

Despite these advancements, the assessment of textile formability remains challenging. Unlike metal forming, which depends on well-defined mechanical and geometrical parameters, textile forming is influenced by multiple factors, including fibre properties (e.g., fibre modulus, yarn density), fabric architecture (e.g., interlacement angles, fibre volume fraction), and fabric geometry (e.g., thickness,

[a]Corresponding author.
E-mail: akdash@outr.ac.in

length). The inherent heterogeneity of textile materials further complicates their forming behaviour, making it essential to develop systematic methods for characterisation[23-25].

Various approaches have been explored to evaluate fabric formability, including numerical, empirical, and statistical modelling[26]. While numerical simulations analyse deformation at the micro level, commercial software cannot often account for complex textile architectures. Empirical methods, on the other hand, require large datasets due to the numerous variables involved, making them time-consuming and expensive. To address these limitations, Yu *et al.*[21] and Cai *et al.*[22] proposed a two-step methodology for 2D woven fabrics, first examining deformation under simple loading conditions and then establishing a functional relationship between deformation modes and overall formability.

Building upon these insights, this study explores the formability of six different 3D orthogonal and interlock structures. Forming energy is considered the primary index for comparison, with all fabrics woven using basic 2D textile designs — plain, matt and twill — while maintaining a constant stuffer-binder ratio (1:1). Further, the study aims to find correlations between bending rigidity, forming energy and fabric crossover points to develop reliable characterisation methods for assessing 3D textile preform formability. The findings will contribute to a deeper understanding of fabric formability, aiding the development of textile structures optimised for advanced composite applications.

2 Materials and Methods

2.1 Materials

Fabric samples were prepared using E-Glass tows of 1200, 600 and 300 tex. The tenacity and initial modulus of the E-glass tows were measured and found to be 5.78 g/denier (CV = 5.95%) and 233 g/denier (CV = 2.92%), respectively. Using the E-Glass tows, 3D orthogonal and interlock structures were fabricated with different weave designs. The fabrics were prepared based on the standard 2D weave designs, namely plain, matt and twill designs. Orthogonal fabrics were prepared as 1×1 plain, 4×4 matt and 4×4 twill designs, coded as W-1, W-2 and W-3, respectively. Interlock fabrics were prepared as 1×1 plain, 1×1 plain without stuffer and 4×4 twill designs, coded as W-4, W-5 and W-6, respectively.

The idealised weave designs were generated using Autodesk Inventor Professional 2014, based on earlier work[27.] Plain, matt and twill weave designs involving binder tows were chosen, with three stuffer layersincluded. These designs were structured to minimise heald shaft usage, thereby reducing fibre damage. Fabric parameters like tow linear densities, ends per metre (epm) inch (epi), picks per metre (ppm) inch (ppi), and stuffer-binder ratio (1:1) were kept the same for W-1 and W-4 to compare the structural differences between interlock and orthogonal fabrics concerning their forming behaviour. The float length was kept at 4 in matt and twill fabrics to achieve the same number of fibres in the z-direction with 1200 tex of binder tows. W-5 was prepared without straight stuffer tows to ascertain their role in forming behaviour. These designs were optimised for stability, firmness, and weavability within a 2D weaving system, wherein the binder tows were solely responsible for maintaining structural integrity.

2.1.1 Weaving of Preform Samples

A 2D weaving machine (CCI Tech Inc., Taiwan) equipped with a separate let-off arrangement for stuffer and binder warp yarns was used. The lifting (peg) plans for all the samples followed previous work[27]. The weaving parameters are given in Table 1.

2.2 Test Methods

2.2.1 Formability Experiments

The experimental plan for testing formability followed the methodology of Cai *et al.*[22]. The experimental set-up is depicted in Fig. 1, showing the plunger position at the beginning and the end of the test. The load-displacement curve during plunger movement was recorded for each sample, and the forming energy was calculated as the area under this curve.

The detailed stepwise process of fabric formation is illustrated in Fig. 2.

2.2.2 Bending Rigidity

The conventional cantilever test for lightweight fabric bending properties was slightly modified to adapt E-glass preforms of higher areal density[28]. The test was conducted using the fixed-angle flexometer method (ISO 4604, 1978). Peirce established a relationship between bending length (c) and bending angle (θ) as per the following equation:

$$c = l\left(\frac{Cos\frac{\theta}{2}}{8tan\theta}\right)^{1/3} \quad ...(1)$$

Table 1 — Weaving parameters of different orthogonal and interlock fabrics

Weave type	W-1	W-2	W-3	W-4	W-5	W-6
N_s, tex	1200	1200	1200	1200	----	1200
N_f, tex	600	600	600	600	600	600
N_b, tex	300	1200	1200	300	1200	1200
Reed count	20	20	20	20	20	20
Denting order	3S/B1/3S/B2	3S/B1/3S/B2/ 3S/B3/3S/B4/ 3S/B5/3S/B6 /3S/B7/3S/B8	3S/B1/3S/B2/ 3S/B3/3S/B4/ 3S/B5/3S/B6 /3S/B7/3S/B8	3S/B1/3S/B2/3S/B3 /3S/B4/3S/B5	B1/B2//B3/ B4//B5	3S/B1/3S/B2/3S/B3/3S /B4/3S/B5/3S/B6/3S/B 7/3S/B8/3S/B9/3S/B10 /3S/B11
EPM of stuffer per layer	198	198	198	198	----	198
EPM of binder	198	198	198	198	396	198
EPM of filler per layer	315	315	315	315	315	315
Width of the fabric, m	0.46	0.46	0.46	0.46	0.46	0.46

N_s, N_f, N_b = Linear density of stuffer, filler and binder, respectively; EPM= Ends per metre

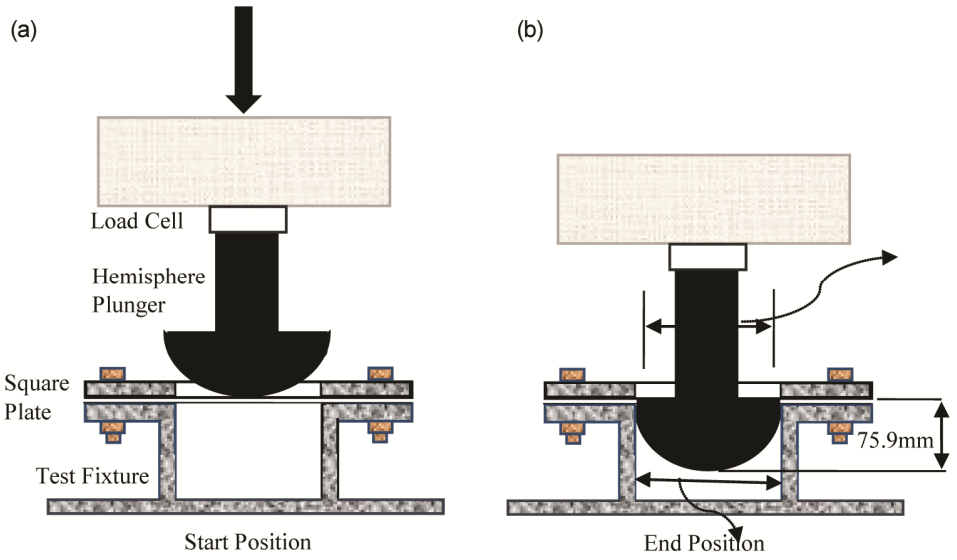

Fig. 1 — Hemispherical plunger (a) at the start of the test, and (b) after completion of the plunger movement

For commercially available equipment with θ=41.5^0, equation (1) simplifies to c' becomes half of 'l'.Flexural or bending rigidity (G) is then calculated using the below equation:

$$G = 0.125\, ml^3 \qquad \ldots(2)$$

where G is flexural rigidity (gm); m, fabric areal density (g/m^2) and l, overhang fabric length.

Equation 2 was proposed for conventional lightweight fabrics (GSM < 200). For heavyweight fabrics (GSM > 200), fixed angle flexometer method was suggested[27], where the bending rigidity was proposed as per the following equation.

$$G = 9.81\, m\, (\tfrac{l}{2}) \qquad \ldots(3)$$

where G is the bending rigidity (mN.m); m, fabric areal density (g/m$^{2)}$; l, average fabric length of overhang (m); and g, acceleration due to gravity (9.81 m/s^2). The additional parameter that is the acceleration due to gravity (g), was taken into account for the calculation of bending rigidity of E-glass fabrics due to their higher areal density.

The same testing procedure was adopted as for conventional fabrics for measuring bending rigidity as per ASTM D1388. Here, the sample size was taken as 35 cm × 35 cm for better dimensional stability. Measurement of the overhanging length was done in the warp and weft directions. Five repetitions were done for each direction of the fabric. Then, the average overhang length was considered to find the

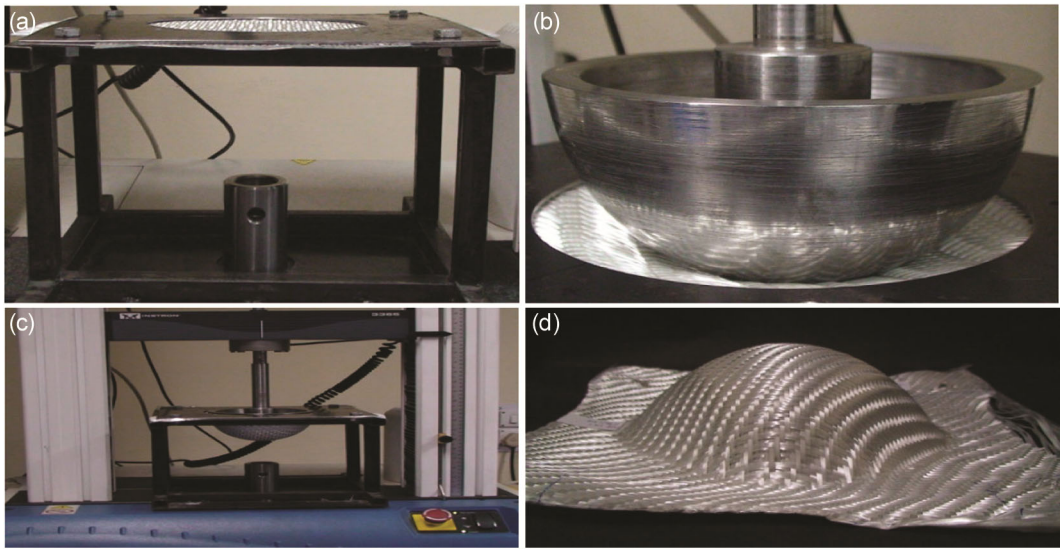

Fig. 2 — (a) Fabric sample mounted in the test frame, (b) hemispherical plunger pressing the fabric, (c) pressing action in Instron 3341 (compression mode) and (d) formed fabric sample after the test

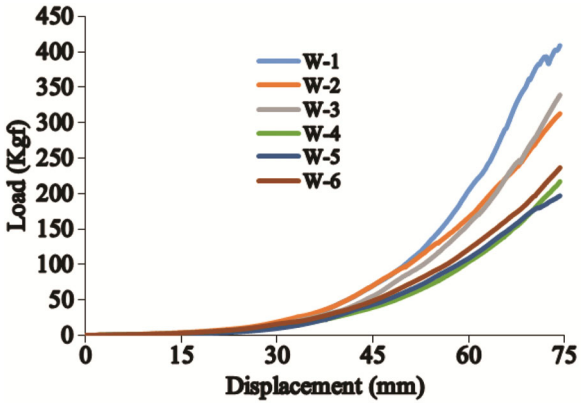

Fig. 3 — Load-displacement curves for different weave designs

bending rigidity both in warp and weft directions. Total bending rigidity of fabric was calculated[29] according to the following equation

$$G = \sqrt{G_{Warp} \times G_{Weft}} \quad ...(4)$$

3 Results and Discussion

3.1 Forming Energy Analysis

The load-displacement curves for all fabric samples up to a defined extension (75 mm) are presented in Fig. 3. It is evident that orthogonal fabrics exhibit higher load-bearing capacity than interlock fabrics at a particular extension level. This behaviour is attributed to fibres' relative movement and rearrangement without significant fibre extension during the forming process. The inter-yarn friction is minimal due to the smoother yarn surface and lower thread density, and the load-bearing capacity is also dependent upon spacing among fibres or yarns. The fibres and yarns progressively achieve new equilibrium conditions under the forming load.

Since the preforms have different fibre architectures, normalisation is needed for a proper comparison. The forming energy (U_f) is defined as the area under the load-displacement curve or, mathematically, the integration of force over displacement. Since all the samples have the same area, only the effect of thickness (h) and fibre volume fraction (V_f) must be considered. When two solid plates of different thicknesses are bent, the thickness effect can be normalised with h^3 as the factor based on the moment/curvature relationship. Similarly, if two fabrics of different thicknesses and fibre volume fractions are bent, the normalisation factor[22] will be $(h.V_f)^3$.

Further, fibre modulus (E_f) is also included as a normalisation factor. Therefore, dimensionless normalised forming energy is calculated as per the following equation[22]:

$$U^*_f = \frac{U_f}{E_f (hV_f)^3} \quad ...(5)$$

The normalised values of forming energy are plotted in Fig. 4.

Among the six 3D weave designs, orthogonal structures exhibit higher forming energy than interlock structures, indicating lower formability. The W-1 weave design consumes the highest energy to

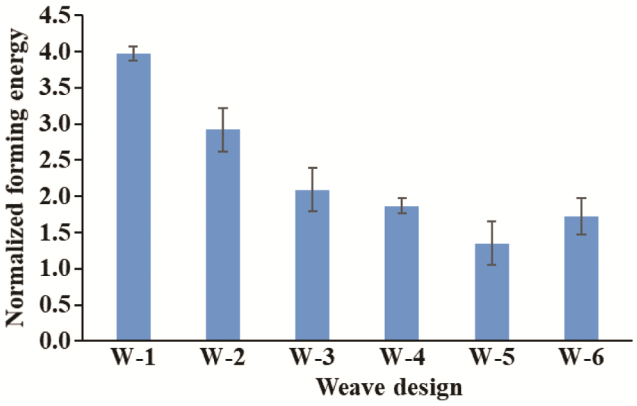

Fig. 4 — Normalised forming energy of different weave designs

form, owing to its regular weave pattern with a higher number of crossovers over a unit area, which restricts fibre movement and repositioning during forming. Conversely, W-5 demonstrates the lowest forming energy due to the absence of straight stuffer tows.

Forming energy serves as a measure of the difficulty of theforming process, with dimensionless normalisation accounting forfibre modulus, fabric thickness, and fibre volume fraction. Other influential factors, such as yarn interlacing density, interlacing angle, yarn diameter and yarn count, are hard to normalise by conventional approaches. Figure. 5 represents the images of the formed samples after the

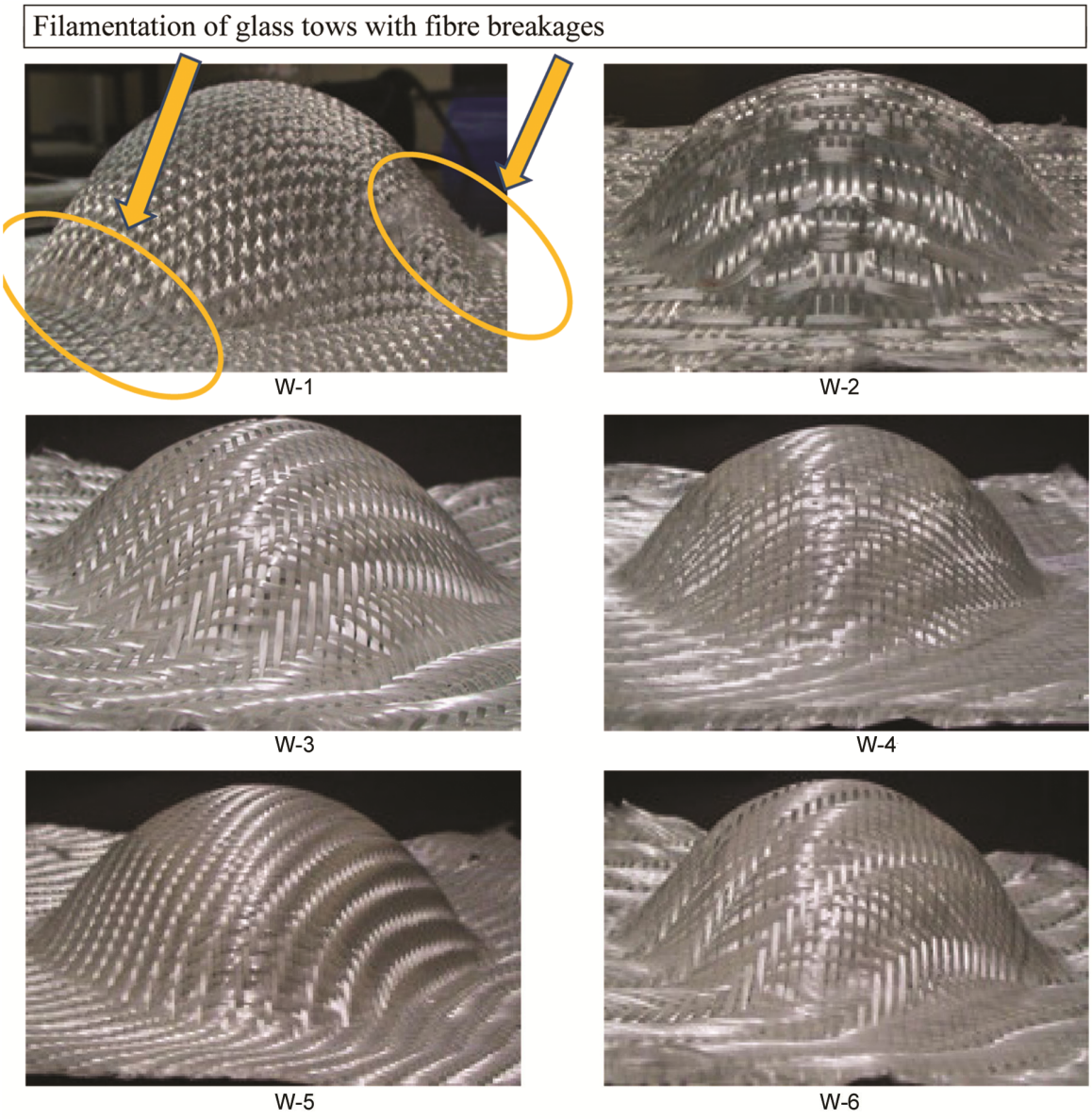

Fig. 5 — Images of the formed samples

Table 2— Bending rigidity values of different orthogonal and interlock fabrics

Weave type	GSM	Bending length, mm (Warp)	Bending rigidity, Nm (Warp)	CV%	Bending length (mm) (Weft)	Bending rigidity (Nm) (Weft)	CV%	Overall bending rigidity, Nm
W-1	1617	75	6685284.4	4.1	65	4356313.2	4.1	5396590.8
W-2	1685	67	4966499.4	9.3	62	3939526.1	8.6	4423308.0
W-3	1850	68	5700652.2	6.6	64	4757520.4	5.5	5207779.6
W-4	1675	62	3912154.1	4.7	60	3549258.0	5.8	3726291.0
W-5	1306	50	1599850.0	13.4	47	1330165.7	10.6	1458789.1
W-6	1812	65	4876680.9	5.7	60	3839555.5	6.1	4327156.9

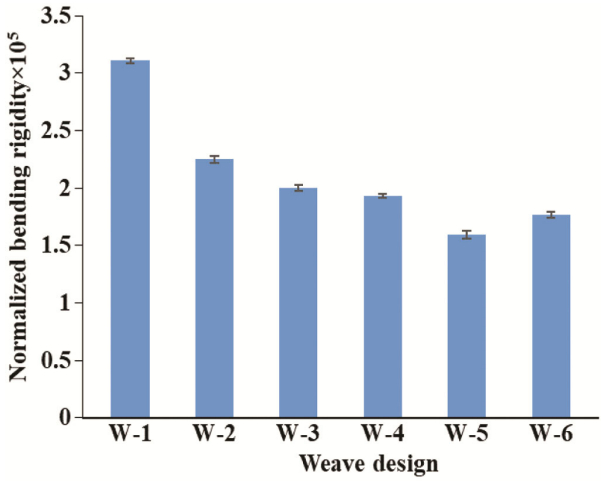

Fig. 6 — Normalised bending rigidity of different weave designs

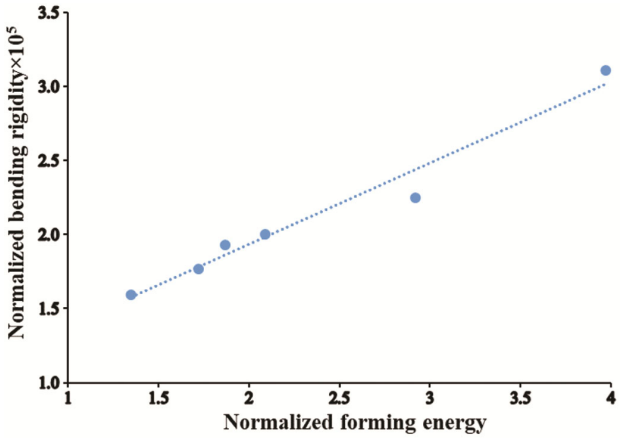

Fig.7 — Normalised forming energy *vs* normalised bending rigidity for different weave designs

test, showing different tow alignment and fibre breakages, as the case may be.

3.2 Bending Rigidity Analysis

The warp and weft bending rigidity values were experimentally determined, and the overall bending rigidity was calculated using Eq. 4 and the detailed data are represented in Table 2.

The overall bending rigidity was further normalised with the fabric thickness and fibre volume fraction to obtain dimensionless values using the following equation, and shown in Fig. 6.

$$G^* = \frac{G}{E_f\,(hV_f)^3} \qquad ...(6)$$

where G^* is the normalised bending rigidity; G, measured bending rigidity; h, thickness of the sample; V_f, fibre volume fraction of the sample; and E_f, fibre elastic modulus.

Figure. 6 reveals that the highest normalised bending rigidity is observed in W-1, likely due to the vertical and consecutive interlacement patterns of the binder tows with the weft tows.In contrast, W-5 shows the lowest normalised bending rigidity, primarilydue to the absence of straight stuffer tows. On the whole, the orthogonal weave designs exhibit higher normalised bending rigidity values in comparison to interlock designs. In interlock weave designs, the angular travel of binder tows results in a more open structure with reduced frictional contact among yarns, thereby lowering bending rigidity.

3.3 Correlation between Forming Energy and Bending Rigidity

The relationship between normalised forming energy and normalised bending rigidity for different weave designs is illustrated in Fig. 7. The results align with findings by Cai *et al.*[22], indicating a strong proportional correlation between forming energy and bending rigidity with a coefficient of determination value of 0.9654. Despite using different fabric samples for formability and bending tests, the averaged results exhibit excellent correlation, suggesting that bending tests can effectively characterise fabric formability for attaining complex shapes.

3.4 Characterisation of Forming Energy and Bending Rigidity with Fabric Crossover Points

Different weave designs of fabrics lead to changes in fabric crossover points. Hence, an attempt has been

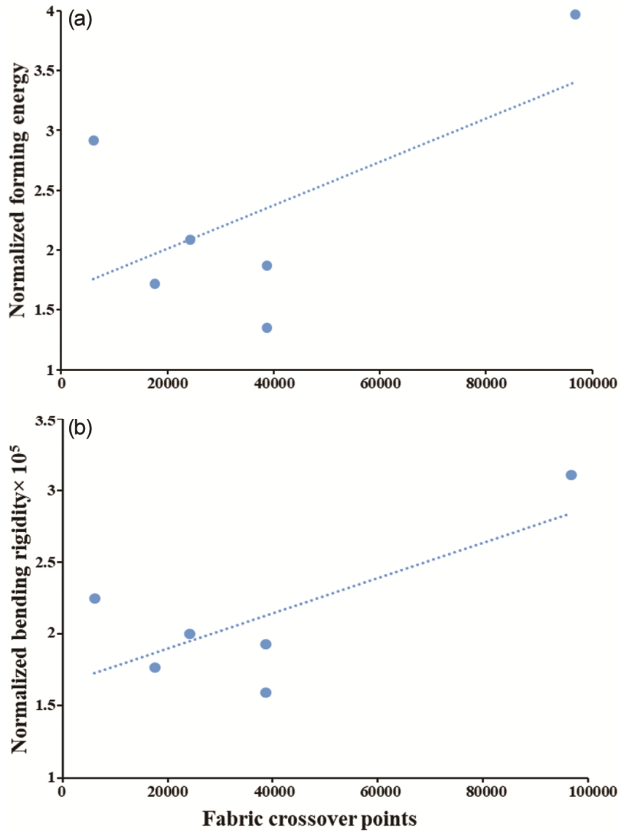

Fig. 8 — (a) Normalised forming energy *vs* fabric crossover points and (b) normalised bending rigidity *vs* fabric crossover points for different weave designs

made to find a correlation between normalised forming energy and normalised bending rigidity with fabric crossover points of different weave designs shown in Fig. 8 (a) and (b), respectively. The coefficient of determination was found to be 0.3611 while relating the former one whereas it was found to be 0.5284 in the latter one.

A reasonably good correlation is observedbetween normalised bending rigidity and normalised forming energy with fabric crossover points, though not as strong as the direct correlation between forming energy and bending rigidity. Additional fabric parameters, such as yarn linear density, thread spacing inside the fabric, thread interlacement angle, fabric length and width, may interfere with the forming energy and bending rigidity results. Nevertheless, fabric crossover points play a major role in deciding the forming energy as well the bending rigidity of the fabric. This is mainly attributed to inter-yarn friction at crossover points, which significantly contribute to the flexural properties of a woven construction, particularly at the initial stage.

4 Conclusion

This study demonstrates the influence of weave design on the forming energy and bending rigidity of 3D woven fabrics. Orthogonal structures exhibit higher forming energy, indicating lower formability compared to interlock structures. The W-1 requires the highest energy to form due to its high crossover density, while W-5 exhibits the lowest forming energy owing to the absence of straight stuffer tows. Similarly, bending rigidity is higher in orthogonal structures, particularly in W-1, due to increased interlacement of binder and weft tows, whereas W-5 shows the least rigidity. A strong correlation between forming energy and bending rigidity is revealed, confirming that bending tests effectively characterise fabric formability. Fabric crossover points significantly influence these properties, though additional parameters such as yarn linear density, thread spacing, and interlacement angle may contribute to variability. The study provides critical insights into optimising fabric architecture for enhanced formability and structural performance, offering valuable guidance for composite material applications.

References

1 Lindberg L, Waesterberg & Svenson R, *J Text Inst Trans*, 51 (12) (1960) T1475, doi: 10.1080/19447026008662578.
2 Saville B P, *Physical Testing of Textiles* (Elsevier) (1999).
3 De-Boos A G & Roczniok A F, *Int J Cloth Sci Technol*, 8 (5) (1996) 51, doi: 10.1108/09556229610151125.
4 Matusiak M & Sikorski K, *J Fibres Text*, 19 (5) (2011) 46.
5 Bogusławska-Baczek M & Hes L, *Fibres Text East Eur*, 97 (1) (2013) 67.
6 Frydrych I, Dziworska G &Matusiak M, *Fibr Text East Eur*, 3 (42) (2003) 31.
7 Sankaran V & Subramaniam V, *Fibres Text East Eur*, 94 (5) (2012) 56.
8 Kim S J, Kim K H, Lee D H & Bae G H,*Int J Cloth Sci Technol*, 10 (3/4) (1998) 273, doi: 10.1108/09556229810693627.
9 Behera B K & Mishra R,*Indian J Fibre Text Res*, 32 (3) (2007) 319.
10 Naujokaitytė L &Strazdienė E, *Change*, 8 (2007) 11.
11 Leung M Y, Lo T Y, Dhingra R C & Yeung K, *Res J Text Appar*, 6 (1) (2002) 39, doi: 10.1108/RJTA-06-01-2002-B004.
12 Long A C, *Design and manufacture of textile composites* (Cambridge Boca Raton by Woodhead CRC), 2005.
13 De Bilbao E, Soulat D, Hivet G & Gasser A, *Exp Mech*, 50 (3) (2010) 333, doi: 10.1007/s11340-009-9234-9.
14 Allaoui S, Boisse P, Chatel S, Hamila N, Hivet G, Soulat D & Vidal-Salle E, *Compos Part A: Appl Sci Manuf*, 42 (6) (2011) 612, doi: 10.1016/J.COMPOSITESA.2011.02.001.
15 Boisse P, *Composite reinforcements for optimum performance* (Woodhead Pub), 2011.

16 Khan M A, Mabrouki T, Vidal-Sallé E & Boisse P,*J Mater Process Technol*, 210 (2) (2010) 378,doi: https://doi.org/10.1016/j.jmatprotec.2009.09.027.
17 Zhu B, Yu T X, Zhang H & Tao X M, *Compos Part B Eng*, 42 (2) (2011) 289, doi: https://doi.org/10.1016/ j. compositesb.2010.05.006.
18 Behera B K & Mishra R, *Indian J Fibre Text Res*, 33 (3) (2008) 274.
19 Khokar N, *J Text Inst*, 92 (2) (2001) 193, doi: 10.1080/00405000108659570.
20 Chen X, Taylor L W & Tsai L J, *Text Res J*, 81 (9) (2011) 932, doi: 10.1177/0040517510392471.
21 Yu J Z, Cai Z, and Ko F K,*Compos Manuf*, 5 (2) (1994) 113, doi: 10.1016/0956-7143(94)90062-0.
22 Cai Z, Yu J Z & Ko F K, *Compos Manuf*, 5 (2) (1994) 123, doi: https://doi.org/10.1016/0956-7143(94)90063-9.
23 Lomov S V, Gusakov A V, Huysmans G, Prodromou A & Verpoest I, *Compos Sci Technol*, 60 (11) (2000) 2083, doi: 10.1016/S0266-3538(00)00121-4.
24 Lomov S V *et al.*, *Compos Part A Appl Sci Manuf*, 32 (10) (2001) 1379, doi: 10.1016/S1359-835X(01) 00038-0.
25 Verpoest I & Lomov S V, *Compos Sci Technol*, 65 (15) (2005) 2563, doi: https://doi.org/10.1016/ j.compscitech. 2005.05.031.
26 Gereke T, Döbrich O, Hübner M & Cherif C, *Compos Part A Appl Sci Manuf*, 46 (1) (2013) 1, doi: 10.1016/ j.compositesa.2012.10.004.
27 Dash A K & Behera B K, *J Text Inst*, 109 (7) (2018) 952.
28 Bilisik K & Yolacan G, *Text Res J*, 82 (10) (2012) 1038.
29 Süle G, *J Eng Fiber Fabr*, 10 (2) (2015) 164, doi: 10.1177/155892501501000219.